Biochimica et Biophysica Acta 1828 (2013) 1205–1213

Contents lists available at SciVerse ScienceDirect

Biochimica et Biophysica Acta

journal homepage: www.elsevier.com/locate/bbamem

Surface pressure induced structural transitions of an amphiphilic peptide in pulmonary surfactant systems by an in situ PM-IRRAS study

Hiromichi Nakahara, Sannamu Lee, Osamu Shibata *

Department of Biophysical Chemistry, Faculty of Pharmaceutical Sciences, Nagasaki International University, 2825-7 Huis Ten Bosch, Sasebo, Nagasaki 859-3298, Japan

ARTICLE INFO

Article history:
Received 9 October 2012
Received in revised form 30 December 2012
Accepted 8 January 2013
Available online 13 January 2013

Keywords:
RDS
Langmuir monolayer
Lung surfactant
DPPC
PG
SP-B

ABSTRACT

Pulmonary surfactant model peptide, Hel 13–5, in binary and ternary lipid mixtures has been characterized employing the polarization–modulation infrared reflection–absorption spectroscopy (PM-IRRAS) in situ at the air–water interface for a monolayer state and the polarized ATR-FTIR for a bilayer film. In the bilayer form, Hel 13–5 predominantly adopts an α-helical secondary structure in the lipid mixtures. It had been made clear from CD measurements that the Hel 13–5 structure is mainly in the α-helical form in aqueous solutions. In the monolayer state, however, the secondary structure of Hel 13–5 exhibits an interconversion of the α-helix into β-sheet with increasing surface pressures. The difference in the secondary structure is attributed to formation of a surface-associated reservoir just below the surface monolayer. The reservoir formation is a key function of pulmonary surfactants and is induced by a squeeze-out of the fluid components in their monolayers. Compression and expansion cycles of the monolayers generate a hysteresis in molecular orientation of the lipid monolayer as well as in peptide structure. The formation and deformation of reservoirs are, in common, deeply related to the hysteresis behavior. Thus, the transition of peptide structures across the interface is a quite important matter to clarify the role and its mechanism of the reservoirs in pulmonary functions. The present study primarily reveals roles of the anionic lipids in control of the peptide secondary structure. Accordingly, it is demonstrated that they prevent the protein structure transition from α-helix into β-sheet by incorporating the peptide during the squeeze-out event.

1. Introduction

Pulmonary surfactant (PS), which lines an air–alveolar fluid interface of mammalian lungs, functions to control surface tension at the interface during breathing and to exert primary immunization against exogenous bacteria and viruses. In particular, the former accomplishes prevention of alveolar collapses at end-expired state and minimization of the work of breathing [1]. The mechanism is based on formation of surface monolayers enriched in dipalmitoylphosphatidylcholine (DPPC) and on that of bilayer or multilayer structures (or surface-associated reservoirs) closely attached to the monolayers at low surface tensions. A variety of investigations utilizing intact lung tissue and model film have demonstrated the existence of surface-associated reservoirs. Schürch et al. reported visually on the existence utilizing transmission electron microscopy [2,3]. In the paper, the surface layer partially integrates a multilayer structure, which consists of 4–7 straight lamellae. Recently, Thomas and co-workers have revealed a multilayer structure of lipid–protein bilayers in porcine lung surfactant system with neutron reflection [4]. In addition, the existence of layered structures has been supported in studies on films that mimic the alveolar lining layer using fluorescence microscopy (FM) and atomic force microscopy (AFM) [5–8]. The layered structure is considered to act as reservoirs for fluid molecules such as surfactant proteins (SP-B and SP-C) and anionic phospholipids (phosphatidylglycerol, or PG). These observations over the past decade engender high confidence in relevance of the reservoirs to the breathing mechanism. However, the structural transition and activity of the reservoirs and their compositions along the compression–expansion cycle remain unknown at the molecular level. A few reports have shown the fact that the formation of reservoirs generates a delay of respreading of the excluded materials onto the surface during film expansion [7,9], which is commonly exhibited as a characteristic of hysteresis loop in a surface pressure (π)—molecular area (A) isotherm. The functions in reservoirs are considered to be related with the fluidity (or solubility) of PS components and with the specific interaction between positively charged proteins and negatively charged PG [7,9,10]. More recently, the electrostatic interaction with charged palmitic acid (PA) utilizing the PS models has been demonstrated [11]. However, it has been hardly discussed how the interaction affects the protein structures and lipid conformations due to the multiformity of PS components. That is, the distinct mechanisms in reservoir functions

* Corresponding author. Tel./fax: +81 956 20 5686.
E-mail address: wosamu@niu.ac.jp (O. Shibata).
URL: http://www.niu.ac.jp/~pharm1/lab/physchem/indexenglish.html (O. Shibata).

0005-2736/$ – see front matter © 2013 Elsevier B.V. All rights reserved.
http://dx.doi.org/10.1016/j.bbamem.2013.01.003

are obscured by a spacial bulkiness of protein structures, their several interaction sites with lipids, and a content of multicomponent lipids.

In most mammals, PS is composed of ~90 wt.% lipids and ~10 wt.% proteins classified as SP-A, SP-B, SP-C, and SP-D. The lipids consist predominantly of phosphatidylcholines (especially DPPC, ~50 wt.%) and of smaller but significant amounts of PG and PA [12–14]. With respect to the proteins, the hydrophobic SP-B has a crucial role in pulmonary functions at the air–alveolar fluid interface [15–17]. SP-B has a net charge of +7 under the physiological condition, which is thought to be essential for electrostatic interactions between its polar residues and the headgroups of negatively charged lipids such as PG [7,10] and PA [11]. In this regard, synthetic peptides based on amino acid sequence of SP-B have been designed to clarify the mechanism of lipid–protein interactions across the interface and to develop synthetic surfactant preparations containing artificial peptides such as KL_4 [18–20] and Hel 13–5 [9,21,22] for the patients suffering from respiratory distress syndrome (RDS). Hel 13–5 is a monomeric synthetic peptide based on N-terminal segment of SP-B. Its structure and surface activity have been systematically investigated from the thermodynamic and morphological aspects [8,21,23]. The secondary structure of Hel 13–5 is predominantly α-helix in aqueous solutions containing phospholipids [24,25]. In the monolayer, however, its structure varies depending on surface pressure and surrounding lipid [26]. Generally, the hysteresis behavior is observed in thermodynamic parameters such as surface pressure and surface potential against molecular area during the compression and expansion cycle. In addition, recent works have showed the hysteresis for secondary structure of peptides employing the IRRAS technique [26–28]. However, it is not still established at the molecular level how the hysteresis behavior is induced, although it is considered to be deeply related with the reservoir formation below the surface.

Herein, we report variational modes of the peptide secondary structure and lipid conformation along the formation and deformation of the reservoirs utilizing PS model preparations. To catch the modes, attenuated total reflectance (ATR)-FTIR and polarization–modulation infrared reflection-absorption spectroscopy (PM-IRRAS) have been employed for bilayers and monolayers in situ at the air–water interface, respectively. PM-IRRAS is almost insensitive to the strong IR absorption of water vapor and allows the extraction of faithful information on conformation and orientation of proteins in the monolayer. It is evident that secondary structure determination of surfactant proteins and their analogue peptides in monolayers is essential for understanding their in vivo function during respiration and for designing model peptides for the replacement therapy. The aims of the present study are to reveal the correlation between the reservoir function and the electrostatic (lipid–peptide) interactions during lateral compression–expansion cycles [9] and to elucidate the secondary structure transfer by applying surface pressure at the air–water interface. ATR-FTIR spectra for the (bilayer) films are utilized to confirm the peak frequency of PM-IRRAS spectra in the amide region and to compare the data accumulated in the aqueous solution with those at the surface. PM-IRRAS spectra of the monolayers are separately analyzed for antisymmetric methylene vibration of the lipids and for the amide I mode of Hel 13–5. Multiple IR data have been collected for PS model preparations of DPPC/PA (=90/9, wt/wt), DPPC/PG (=68/22, wt/wt), and DPPC/PG/PA (=68:22:9, wt/wt/wt) with or without Hel 13–5 under the physiological condition [9]. The ternary DPPC/PG/PA mixture mimics the lipid compositions existing in amnion liquid and has been used for synthetic-type RDS medicine such as Surfaxin® and preparations [19,29–31].

2. Materials and methods

2.1. Materials

Hel 13–5 (NH_2-KLLKLLLKLWLKLLKLLL-COOH, >98%) peptide was synthesized by the Fmoc (9-fluorenylmethoxycarbonyl) technique and purified with reverse-phase HPLC as described elsewhere [24]. Detailed procedures of synthesis, purification, and basic analysis for Hel 13–5 were reported previously [25,32]. L-α-Dipalmitoylphosphatidylcholine (DPPC; purity >99%) and L-α-phosphatidylglycerol (PG; purity >99%) were obtained from Avanti Polar Lipids, Inc. (Alabaster, AL). PG was supplied as its sodium salt (egg, chicken). Palmitic acid (PA, purity >99%) was purchased from Sigma (St. Louis, MO). These lipids were used without further purification. Chloroform (99.7%) and methanol (99.8%) used as spreading solvents were purchased from Cica-Merck (Uvasol, Tokyo, Japan) and nacalai tesque (Kyoto, Japan), respectively. Tris(hydroxymethyl) aminomethane (Tris) and acetic acid (HAc) of guaranteed reagent grade for the preparation of a subphase were obtained from nacalai tesque. Sodium chloride (nacalai tesque) was roasted at 1023 K for 24 h to remove all surface-active organic impurities. The substrate solution was prepared using thrice distilled water (the surface tension = 71.96 mN m^{-1} at 298.2 K and the electrical resistivity = 18 MΩcm).

2.2. Langmuir monolayer preparations

Stock solutions of DPPC (1.0 mM), PG (0.5 mM), PA (1.0 mM), and Hel 13–5 (0.1 mM) were prepared in chloroform/methanol (2/1, v/v). In the present work, we used the following three model lipids as pulmonary surfactant (PS) lipids; the binary DPPC/PA (=90/9, wt/wt), binary DPPC/PG (=68/22, wt/wt), and ternary DPPC/PG/PA mixtures. For the PS model preparations, the lipids with a constant but critical amount of Hel 13–5 ($X_{\text{Hel 13–5}} = 0.1$) were utilized, because the peptide concentrations strongly affect the phase behavior [9,21] and spectrum mode [26,27] of PS preparations. Detailed information on lipid and peptide compositions was described in the previous study [21]. An aliquot of the solutions is spread onto the subphase of 0.02 M Tris buffer with 0.13 M NaCl (pH 7.4). The preparation of the subphase was performed as described previously [21,23]. The spreading solvents were allowed to evaporate for 30 min prior to compression for PM-IRRAS measurements. The monolayer was compressed and expanded at a speed of <0.11 nm^2 $molecule^{-1}$ min^{-1}. The temperature was kept constant at 298.2 ± 0.1 K throughout the experiments.

2.3. ATR-FTIR measurements

Polarized ATR-FTIR spectra were recorded on a Fourier transform spectrometer (JASCO FT/IR-4200, Tokyo, Japan) at a nominal resolution of 2 cm^{-1}. A horizontal ATR accessory (ATR PRO410-S, JASCO) was used with a germanium crystal (Ge, refractive index = 4.0) as an internal reflection element (IRE). The angle of incidence of the IRE was 45° (single reflection). The surface of the ATR crystal available for coating by the sample (refractive index = 1.4 [33,34]) had dimensions of 1.8 mm^2. A zinc selenide (ZnSe)-mounted IR holographic wire-grid polarizer with the diameter of 25 mm (Edmund Optics, NJ, USA) was used in the incident beam to control both p- (parallel to the plane of incidence) and s- (perpendicular) polarization. A total of 512 individual scans were co-added at room temperature. The spectrometer was purged with dry air (1.0 L/min). Aliquots (30 μL) of ~0.5 mg/mL $CHCl_3$/MeOH (=2/1, v/v) solutions of the desired sample composition were dried down on the Ge ATR crystal. After evaporation of the solvents, spectra of the dry sample (not hydrated vesicles) were recorded with the polarized (p and s) and non-polarized radiation. Data analyses of the phosphate stretching (1000–1300 cm^{-1}), the amide (1400–1800 cm^{-1}), and the methylene stretching (2800–3000 cm^{-1}) regions were accomplished with Spectra Manager Ver. 2 (JASCO). The spectra displayed in the figures were the mean spectra of at least 3 runs.

The order parameter of an α-helical peptide in a supported film can be derived from the measured dichroic ratio (R^{ATR}) in the spectral region 1662–1645 cm^{-1} [35]. This ratio was then used to calculate the following molecular order parameter (S) of the

peptide [33]:

$$S = \frac{2}{3\cos^2\alpha - 1} \cdot \frac{E_x^2 - R^{ATR}E_y^2 + E_z^2}{E_x^2 - R^{ATR}E_y^2 - 2E_z^2} \quad (1)$$

where E_x, E_y, and E_z denote the normalized electric field components when the IR beam is polarized in the respective directions; $E_x = 1.411$, $E_y = 1.461$, and $E_z = 0.770$ are used in the present study [36]. For the peptide, the angle (α) between the helix axis and the transition dipole moment was typically fixed at 39° [33,37–40]. In addition, S was also calculated using the following equation;

$$S = \frac{3\cos^2\theta - 1}{2} \quad (2)$$

where θ is the mean angle between the helix axis and the membrane normal, namely the mean tilt angle of α-helix backbone against the direction perpendicular to the IRE surface. More details were described in the previous study [26].

2.4. PM-IRRAS measurements

In situ polarization–modulation infrared reflection–absorption spectrum (PM-IRRAS) measurements at the air–water interface were performed using a KSV PMI 550 instrument (KSV Instruments Ltd., Helsinki, Finland) coupled to a commercially available film balance system (KSV Minitrough, KSV Instruments Ltd.). The incident angle at 80° relative to the normal of the air–water interface was selected in the present study. The total acquisition time for each spectrum was 5 min, resulting in 3000 interferograms per spectrum. The spectral range of the PMI 550 device is 800–4000 cm^{-1}, and the resolution is 8 cm^{-1}. The details on the apparatus and experimental parameters were described previously [26,41]. PM-IRRAS spectra were acquired, while the monolayer is held at selected surface pressures during step-wise compression and expansion. The raw PM-IRRAS spectrum is obtained in the form of $\Delta I = (I - I_0)/I_0$, where I_0 is the signal of the bare water surface and I is that of the film-covered surface. All the spectra were normalized by subtracting base line spectra from the raw spectra. The spectra displayed in the figures were the mean spectra of 5 runs. Spectra were subjected to second-derivative and curve-fitting procedures in order to fit the amide I and II bands in the region 1400–1800 cm^{-1} with a Gaussian band shape, using PeakFit software (ver. 4.12, SeaSolve Software Inc., CA, USA). Fitting was judged acceptable when the value of coefficient for the determination between the simulated and the experimental (original) spectra was more than 0.99. The nonlinear curve fitting analysis provided information on peak intensity, peak position, full width at half height (FWHH), and integrated peak area for the Gaussian components in the amide region.

3. Results

3.1. Polarized ATR-FTIR spectra in the amide region

Fig. 1 shows polarized ATR-FTIR spectra of dry films of DPPC/PA (=90/9, wt/wt)/Hel 13–5, DPPC/PG (=68/22, wt/wt)/Hel 13–5, and DPPC/PG/PA (=68:22:9, wt/wt/wt)/Hel 13–5 systems at the fixed molar ratio ($X_{Hel\ 13-5} = 0.1$) in 1400–1800 cm^{-1}, where the amide I (1600–1700 cm^{-1}) and II (1500–1600 cm^{-1}) regions are involved. Two positive bands at ~1650 (amide I) and ~1545 (amide II) cm^{-1} are assigned to intense bands regarding peptide amide groups (C=O and N−H, respectively). It is well established that frequency and shape of the amide band depend critically on secondary structure of peptide and protein films [34,37,42]. Secondary structure of Hel 13–5 alone in the dry-film form was confirmed to be completely α-helix; two positive bands at 1656 (amide I) and 1541 (amide II) cm^{-1} [26]. In the DPPC/PA/Hel 13–5 spectra, four major peaks are observed at ~1740, 1650, 1545, and 1465 cm^{-1}. The peaks at ~1740 and ~1465 cm^{-1} are assigned to the C=O stretching and CH_2 bending vibrations of the lipids, respectively. Both the amide bands are indicative of the α-helix. A p-polarized spectrum is wholly larger in peak intensity than a s-polarized one. The difference in absorbance between the p- and s-polarized incident radiation means tilted or oriented molecular backbone to the Ge surface. Thus, in common, the difference which is related to a dichroic ratio (R^{ATR}) allows us to calculate the tilt angle of molecular backbones and hydrophobic chains for Hel 13–5 and the lipids, respectively. As for the DPPC/PG/Hel 13–5 and DPPC/PG/PA/Hel 13–5 systems, the spectra are quite similar in peak position to those of the DPPC/PA/Hel 13–5 system. Therefore, the ATR-FTIR spectra in the amide I and II regions suggest that the secondary structure of Hel 13–5 is predominantly the α-helix irrespective of surrounding lipid species.

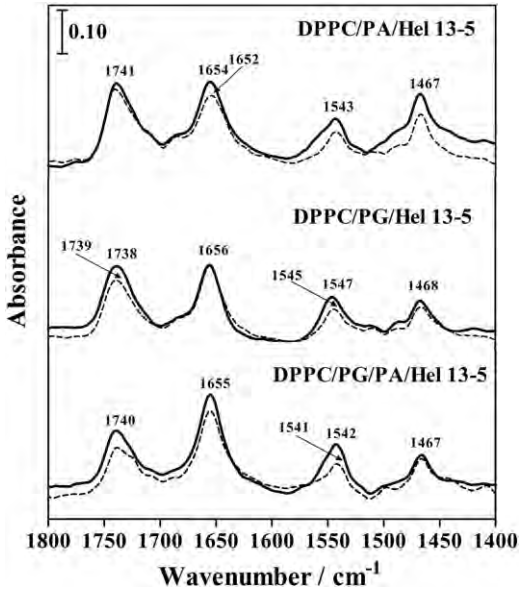

Fig. 1. Polarized ATR-FTIR spectra of a film of the DPPC/PA(=90/9, wt/wt)/Hel 13–5 (upper), DPPC/PG(=68/22, wt/wt)/Hel 13–5 (middle), and DPPC/PG/PA(=68/22/9, wt/wt/wt)/Hel 13–5 (lower) systems at $X_{Hel\ 13-5} = 0.1$ in the region of 1400–1800 cm^{-1} at a room temperature. Solid lines correspond to p-polarization and dashed lines to s-polarization of the incident radiation.

An average tilt angle (θ) of Hel 13–5 α-helical backbone is assessed to gain a better understanding of a dependency of the angle (or the orientation) on the surrounding lipid species. Unfortunately, the peak intensity of PM-IRRAS spectra at the air–water interface is somewhat lower due to the low surface concentration of Hel 13–5 monolayers. Therefore, the tilt angle calculated from the ATR spectra is utilized to discuss the orientation in the present study. The previous work has revealed that the tilt angle for pure Hel 13–5 films is ~59° against a normal to the surface [26]. This value means that the Hel 13–5 backbone is oriented almost parallel to the plane of the Ge surface like a peripheral membrane protein. In the presence of the DPPC/PA, DPPC/PG, and DPPC/PG/PA mixtures, the Hel 13–5 α-helical backbone tilts down on the plane of the surface: $\theta = 70 \pm 9°$, $73 \pm 9°$, and $63 \pm 10°$, respectively. However, the tilt angle (~58°) in the binary DPPC/Hel 13–5 film is almost the same as that in the absence of lipids [26]. That is, it is found that there exist few effective interactions between DPPC and Hel 13–5, which possesses net positive charges (+5). That is, negatively charged PA and PG have a meaningful influence on orientation of the Hel 13–5 secondary structure due to the electrostatic interaction between them. In particular, considering the amphiphilic structure of Hel 13–5 [23,24], the attractive

force of PA and/or PG headgroups with hydrophilic moieties of Hel 13–5 is possible to account for the reinforcement of its tilt angle.

Non-polarized ATR-FTIR spectra of the DPPC/PA (=90/9, wt/wt), DPPC/PG (=68:22, wt/wt), and DPPC/PG/PA (=68:22:9, wt/wt/wt) films with (solid line) or without Hel 13–5 (dotted line) in 1000–1300 cm^{-1} are shown in Fig. 2. The spectra in this region reflect phosphate stretching bands of phospholipid headgroups. Under the present condition, the headgroups of PG and PA are in completely and partially anionic forms, respectively [11]. Accordingly, the charged headgroups are possible to interact with positively charged moieties of Hel 13–5 in the monolayer state [9,11]. The spectra for the whole systems have several bands; mainly, asymmetric PO_2 stretching at ~1240 cm^{-1} [36,43], C—N stretching at ~1200 cm^{-1} [36], asymmetric CO–O–C stretching at ~1175 cm^{-1} [44], symmetric PO_2 stretching at ~1090 cm^{-1} [36,43], and symmetric CO–O–C stretching vibrations at ~1065 cm^{-1} [44]. The ternary systems exhibit few differences in peak frequency between the spectra in the absence and the presence of Hel 13–5. However, in the case of the DPPC/PG/PA/Hel 13–5 film, the two bands at 1066 and 1088 fuse into a band at 1081 cm^{-1} with an obscure shoulder by the addition of Hel 13–5. In common, it is widely accepted that if the charged phosphate group is protonated or protected by other cations, the absorption peak shifts to lower wavenumber [44]. Indeed, in the binary DPPC/Hel 13–5 system, there are no noteworthy interactions between the phosphate group of DPPC and Hel 13–5 from the spectroscopic aspect [26]. In the previous studies, the specific interaction between Hel 13–5 and the lipids with negatively charged headgroups has been reported in terms of thermodynamics and morphological observation [9,11]. Thus, considering that the peak shift and fusion do not occur in the ternary systems here, it is suggested that the presence of PA in the four-component system cooperatively promotes the specific interaction between PG and Hel 13–5.

3.2. In situ PM-IRRAS spectra in the amide region

In previous studies, the behavior of secondary structure for single Hel 13–5 monolayers was clarified using the in situ PM-IRRAS at the air–water interface [26] and their isothermal analyses were made systematically [8,23]. Hel 13–5 in the monolayer state assumes a predominant α-helix secondary structure, which is oriented almost parallel to the surface. After the monolayer collapse over ~42 mN m^{-1}, a structural interconversion from the α-helix to β-sheet is induced. Normalized PM-IRRAS spectra in the region of 1400–1800 cm^{-1} for the DPPC/PA (=90/9, wt/wt) monolayer containing Hel 13–5 ($X_{Hel\ 13-5}$= 0.1) on 0.02 M Tris buffer with 0.13 M NaCl (pH 7.4) are shown in Fig. 3 at different surface pressures (π) during compression (solid line) and expansion (dotted line). The isothermal analysis for the DPPC/PA/Hel 13–5 system was reported previously (see Fig. S1 in the Supporting Materials) [8,11]. The spectra include a broad negative band at 1700—1640 cm^{-1}, which is assigned to $\delta(OH_2)$ deformation vibration mode of the liquid water. However, detailed argument about the band is not done in the present study. There are three positive peaks at ~1611, ~1643, and ~1650 cm^{-1} and one negative peak at ~1682 cm^{-1} in the amide I region. A pair of the peaks at ~1611 and ~1682 cm^{-1} is characteristic of an antiparallel β-sheet for proteins [45–47]. The peak at ~1643 is assigned to a hydrated α-helix induced by surrounding water molecules [28,46]. Both the characteristics of α-helix and β-sheet structures are also seen in the amide II region (1545 and 1525 cm^{-1}, respectively). According to surface selection rules of the PM-IRRAS experiment at the air–water interface, positive absorption bands in the spectrum reflect IR transition dipole moments which are aligned parallel to the interface [48]. Therefore, the α-helical backbone of Hel 13–5 in the DPPC/PA monolayer is found to be oriented parallel to the surface. Upon compression from 5 to 60 mN m^{-1}, the peak assigned to α-helix shifts to lower frequency of ~1643 cm^{-1} and the pair of peaks corresponding to the β-sheet is intensified. On the other hand, during expansion, the β-sheet marker band at 45 mN m^{-1} becomes quite smaller in peak intensity compared with that at the same pressure during compression. This quick restoration of the intensity supports a large hysteresis in surface pressure (π)—molecular area (A) isotherms for pulmonary surfactant preparations [8,21]. Thus, it is suggested that the recovery of secondary structure of pulmonary surfactant proteins such as SP-B and SP-C may be deeply related to the isothermal hysteresis.

Figs. 4 and 5 are the PM-IRRAS spectra of the DPPC/PG (=68/22, wt/wt) and DPPC/PG/PA (=68:22:9, wt/wt/wt) monolayers at $X_{Hel\ 13-5}$= 0.1, respectively. The π—A isotherms for the two systems were reported previously as a function of Hel 13–5 amount under the same condition (see Fig. S1) [8,21]. For the both monolayers, the intensity of the β-sheet marker bands near 1610 cm^{-1} increases with increasing surface

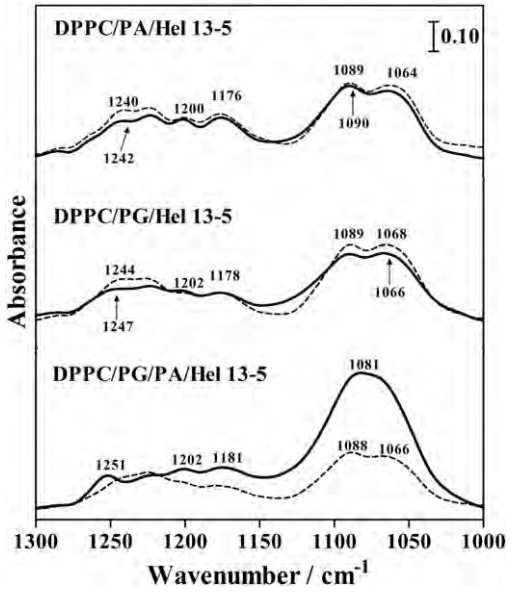

Fig. 2. Non-polarized ATR-FTIR spectra of a film of the DPPC/PA(=90:9, wt/wt)/Hel 13–5 (upper), DPPC/PG(=68:22, wt/wt)/Hel 13–5 (middle), and DPPC/PG/PA(=68:22:9, wt/wt)/Hel 13–5 (lower) systems in the region of 1000–1300 cm^{-1} at a room temperature. Solid lines correspond to the spectra in the presence of Hel 13–5 ($X_{Hel\ 13-5}$=0.1) and dashed lines to the spectra in the absence of Hel 13–5 ($X_{Hel\ 13-5}$=0).

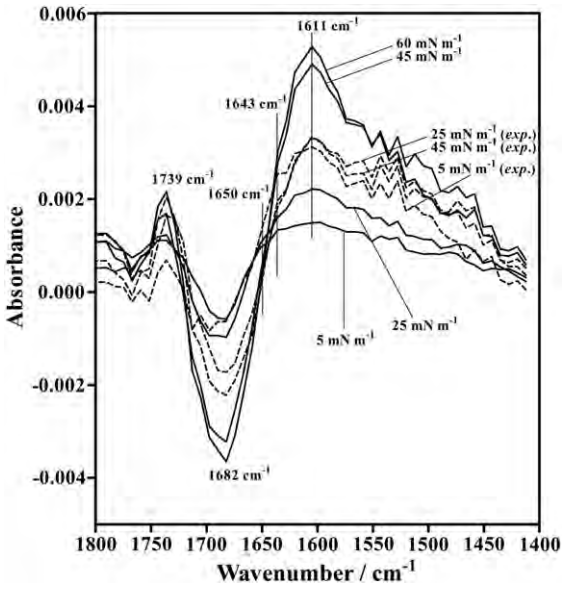

Fig. 3. In situ normalized PM-IRRAS spectra of monolayers of the DPPC/PA(=90:9, wt/wt)/Hel 13–5 system at $X_{Hel\ 13-5}$=0.1 at different surface pressures (π) during compression (solid lines) and successive expansion (dashed lines, *exp.*) in the region of 1400–1800 cm^{-1} on 0.02 M Tris buffer with 0.13 M NaCl (pH 7.4) at 298.2 K.

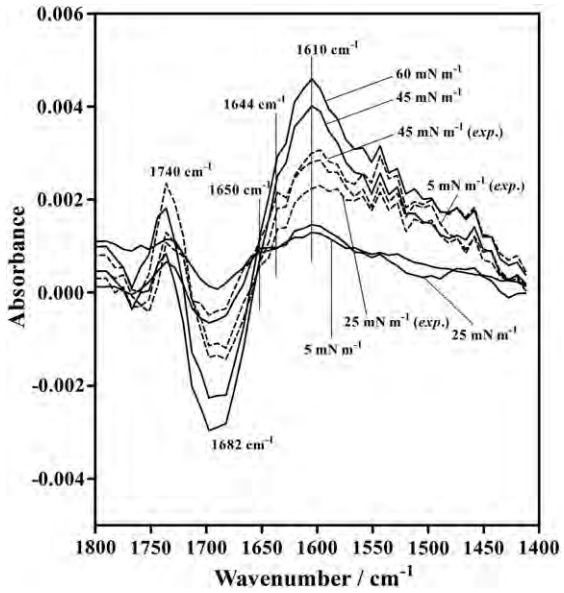

Fig. 4. In situ normalized PM-IRRAS spectra of monolayers of the DPPC/PG(=68:22, wt/wt)/Hel 13–5 system at $X_{\text{Hel 13–5}}=0.1$ at different surface pressures (π) during compression (solid lines) and successive expansion (dashed lines, *exp.*) in the region of 1400–1800 cm^{-1} on 0.02 M Tris buffer with 0.13 M NaCl (pH 7.4) at 298.2 K.

pressures upon compression, similarly to the DPPC/PA/Hel 13–5 preparation (Fig. 3). In addition, the peak assigned to the hydrated α-helix is emphasized in intensity at the expense of the α-helix marker bands at ~1650 cm^{-1}. It is noticed that this shift of peak frequency by ~10 cm^{-1} is observed more clearly in the four-component system (Fig. 5). This implies the cooperative effect of PA and PG on Hel 13–5 secondary structures. During successive expansion processes, the spectrum behavior for the DPPC/PG/Hel 13–5 system (Fig. 4) resembles that for the DPPC/PA/Hel 13–5 system (Fig. 3). As for the DPPC/PG/PA monolayer, however, the peak intensity at ~1610 cm^{-1} is somewhat higher compared with the other systems. That is, the intensity remains high even upon monolayer expansion, which also supports the cooperative interaction of charged PG and PA with Hel 13–5.

3.3. In situ PM-IRRAS spectra in lipid stretching vibration modes

The normalized PM-IRRAS spectra in the region of 2820–2980 cm^{-1} for the DPPC/PG/PA/Hel 13–5 monolayers at $X_{\text{Hel 13–5}}=0.1$ at different surface pressures (π) during compression (solid line) and expansion (dotted line) are exhibited in Fig. 6. The spectra for the other systems show the similar behavior (Fig. S2). The peaks observed in the region commonly catch stretching vibrations of methylene and methyl groups for lipids. There are three kinds of specific peaks of the lipids such as a symmetric methylene stretching vibration (or $\nu_s(CH_2)$) at ~2850 cm^{-1}, an asymmetric methylene stretching vibration (or $\nu_a(CH_2)$) at ~2920 cm^{-1}, and a methyl stretching vibration (or $\nu(CH_3)$) at ~2950 cm^{-1}. Among the three, the $\nu_a(CH_2)$ peak is, in common, larger in intensity and is more sensitive to external stimuli such as lateral compression and temperature. Therefore, the $\nu_a(CH_2)$ mode allows us to probe changes in surface concentration and orientation of the lipid components. The intensity of $\nu_a(CH_2)$ modes increases with an increase in surface pressure and subsequently decreases during the expansion cycle. It is noticed that the $\nu_a(CH_2)$ peak at 45 mN m^{-1} during compression (~0.0075) is considerably different in intensity from that during expansion (~0.0050). At 5 and 25 mN m^{-1}, however, the peak intensities of the $\nu_a(CH_2)$ mode upon monolayer expansion return nearly to the original intensities. In addition, the similar behavior is reflected in the $\nu_s(CH_2)$ modes at ~2850 cm^{-1}. The delay of peak intensity during expansion does not occur in the absence of Hel 13–5 [49]. At higher surface pressures beyond 42 mN m^{-1}, Hel 13–5 is squeezed out of the interface to form a surface-associated reservoir just below the lipid monolayer [9,23]. Thus, these results indicate a possibility that the hysteresis behavior of hydrophobic-chain orientation of the lipids could be related with the formation of surface-associated reservoirs.

The $\nu_a(CH_2)$ RA intensity at ~2920 cm^{-1} for the DPPC/PA/Hel 13–5, DPPC/PG/Hel 13–5, and DPPC/PG/PA/Hel 13–5 at $X_{\text{Hel 13–5}}=$ 0.1 during compression (solid line with filled circles) and expansion (dashed line with open circles) is plotted against surface pressure (Fig. 7). Upon compression, the RA value increases as surface pressures increase and finally reached 0.0067 for DPPC/PA/Hel 13–5, 0.0055 for DPPC/PG/He 13–5, and 0.0087 for DPPC/PG/PA/Hel 13–5 at 60 mN m^{-1}. Considering the maximum $\nu_a(CH_2)$ RA intensity (~0.004) for the binary DPPC/Hel 13–5 system at $X_{\text{Hel 13–5}}=0.1$

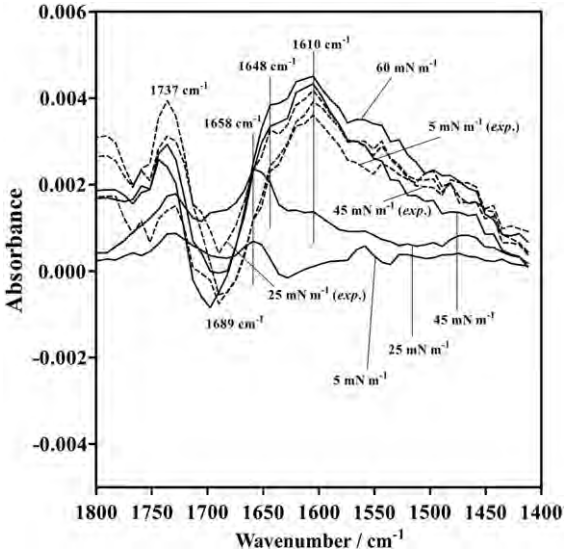

Fig. 5. In situ normalized PM-IRRAS spectra of monolayers of the DPPC/PG/PA(=68:22:9, wt/wt/wt)/Hel 13–5 system at $X_{\text{Hel 13–5}}=0.1$ at different surface pressures (π) during compression (solid lines) and successive expansion (dashed lines, *exp.*) in the region of 1400–1800 cm^{-1} on 0.02 M Tris buffer with 0.13 M NaCl (pH 7.4) at 298.2 K.

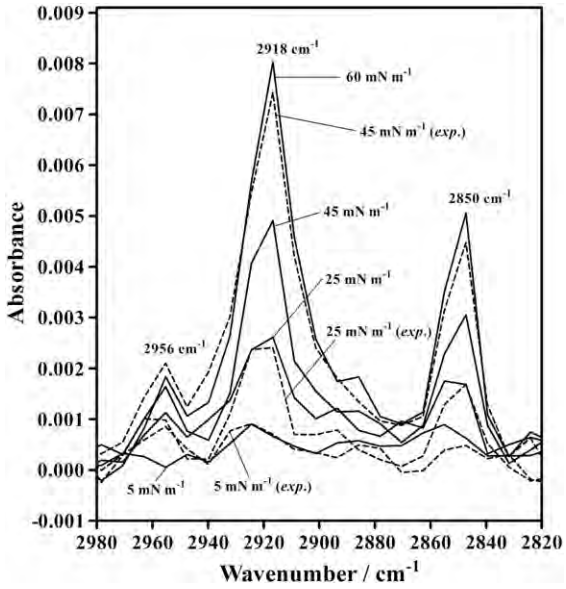

Fig. 6. In situ normalized PM-IRRAS spectra of monolayers of the DPPC/PG/PA(=68:22:9, wt/wt/wt)/Hel 13–5 system at $X_{\text{Hel 13–5}}=0.1$ at different surface pressures (π) during compression (solid lines) and successive expansion (dashed lines, *exp.*) in the region of 2820–2980 cm^{-1} on 0.02 M Tris buffer with 0.13 M NaCl (pH 7.4) at 298.2 K.

[26], all the systems here indicate larger RA values, which means an increase in surface concentration (or density) of aliphatic chains induced by the addition of PA and PG. During the expansion stage, the RA intensity decreases with reducing surface pressures. Nevertheless, all the systems exhibit hysteresis in intensity during the compression and expansion process. The hysteresis regarding the orientation of hydrophobic chains in lipid components is also supported by a surface potential (ΔV) measurement against surface concentration of PS preparations [9]. The ΔV value is related with dipole moment perpendicular to the surface in the Helmholtz equation and thus reflects the monolayer orientation. As for the DPPC/PA/Hel 13–5 system (Fig. 7a), RA intensities under the expansion state from 60 down to 10 mN m^{-1} are kept larger compared with those at the same surface pressures during compression. On the other hand, in the systems containing PG (Fig. 7b and c), RA intensities upon expansion restore to the initial value down by 25 mN m^{-1}. These results suggest that the addition of PA and PG accelerates monolayer packing at high surface pressures during compression and respreading of tightly packed monolayers during the expansion, respectively. This is supported by the plot for the DPPC/PG/PA/Hel 13–5 system, too (Fig. 7c). It has been widely accepted that besides the RA intensity, a wavenumber (or peak frequency) of $\nu_a(CH_2)$ modes for lipid monolayers is much influenced on packing, orientation, and conformational change of their hydrophobic chains and that the wavenumber near 2920 cm^{-1} is characteristic of all-trans conformations of them [43,50,51]. Similarly to the plots in Fig. 7, the wavenumber of $\nu_a(CH_2)$ modes for the DPPC/PA/Hel 13–5 system indicates a hysteresis loop during the cycle, whereas the hysteresis is not be induced for the DPPC/PG/Hel 13–5 system (data not shown). The hysteresis against wavenumber also indicates the condensing effect of PA on the monolayer, which prevents it from respreading during expansion. On the other hand, it is found that the packed chains of lipid monolayers recover upon expansion in the presence of PG.

3.4. Secondary structure transition of Hel 13–5

An α-helix ratio of Hel 13–5 relative to the (α-helix + β-sheet) component for the DPPC/PA (=90:9, wt/wt)/Hel 13–5, DPPC/PG (=68:22, wt/wt)/Hel 13–5, and DPPC/PG/PA (=68/22/9, wt/wt/wt)/Hel 13–5 monolayers at $X_{Hel\ 13-5}=0.1$ during the compression (solid line with filled circles) and expansion (dashed line with open circles) cycle is plotted against surface pressure in Fig. 8. The ratio are calculated from integrated peak areas of the α-helix (~1650 cm^{-1}) and of the β-sheet (~1620 cm^{-1}) marker bands (Gaussian bands) in the amide I region (Figs. 3–5); the ratio $\alpha/(\alpha+\beta)$ means the peak area ratio of amide I band intensities for ~1650 cm^{-1}/(~1650 + ~1620) cm^{-1} [26,27]. In the DPPC/PA/Hel 13–5 system (Fig. 8a), the percentage of the α-helical component decreases from 30 − 40% down to 20% with increasing surface pressures upon compression. During the subsequent expansion process, the ratio rapidly restores to the initial values of 30 − 40%, where hysteresis behavior is observed at higher surface pressures. As for the DPPC/PG/Hel 13–5 system (Fig. 8b), the α-helix ratio sustains the almost constant value of 40% up to 35 mN m^{-1} and then decreases down to 30% during compression. The subsequent expansion of monolayers induces a gradual recovery of the α-helix ratio. The α-helix ratio for the DPPC/PG/PA/Hel 13–5 system seems to be the combined behavior of the two ternary systems (Fig. 8c). The initial α-helix ratio at 5 mN m^{-1} is larger compared to the ternary systems, which means that destruction of hydrogen bonding of Hel 13–5 secondary structures are disturbed by PG components. That is, a fluidizing effect of PG on monolayers results in keeping lipid aliphatic chains away from Hel 13–5. Further lateral compression reduces the α-helix percentage down to 30%. During the expansion process, a sudden return to 40 − 50% of the ratio is observed similarly to the DPPC/PA/Hel 13–5 system. These results indicate that PA and PG components play an important role in the inhibition and recovery of the interconversion of Hel 13–5 secondary structure during the cycles.

4. Discussion

The key function in pulmonary surfactants (PS) at the air–alveolar fluid interface is a squeeze-out process, by which selective exclusions of the fluid components from monolayers are induced at the collapse pressure of the fluid protein monolayers so that the surface film at high surface pressures is enriched in DPPC [52,53]. At that time, it is improbable that organized multilayers are formed as a repository for the excluded material. The surface reservoir is located just below the monolayer and enables the excluded molecules to respread onto the interface upon subsequent expansion [7]. As mentioned in the Introduction, the recent investigations of surface-associated reservoirs by several groups suggest their relevance for the breathing mechanism. It is well-known that the release of squeezed-out molecules from the reservoirs is facilitated by proteins (or peptides). Thus, the composition and molecular structure of the reservoirs are issues of central importance. The PM-IRRAS measurement treated here provides information on molecular structure of the mimicking peptide (Hel 13–5) of SP-B in the presence of the anionic lipids. SP-B and SP-C of hydrophobic proteins have been studied for several decades. However, the change in protein structure including α-helix and β-sheet across the interface and their interaction site with lipid

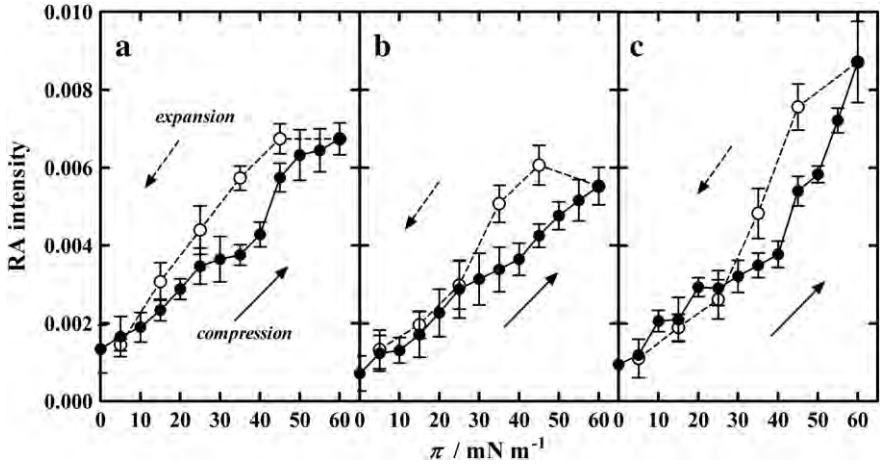

Fig. 7. RA intensity of the asymmetric CH_2 stretching vibrations, $\nu_a(CH_2)$, of lipids in the PM-IRRAS spectra at different surface pressures (π) during compression (filled circles and solid lines) and successive expansion (open circles and dashed lines) for the DPPC/PA(=90:9, wt/wt)/Hel 13–5 (a), DPPC/PG(=68:22, wt/wt)/Hel 13–5 (b), and DPPC/PG/PA(=68:22:9, wt/wt/wt)/Hel 13–5 (c) monolayers at $X_{Hel\ 13-5}=0.1$ on 0.02 M Tris buffer with 0.13 M NaCl (pH 7.4) at 298.2 K.

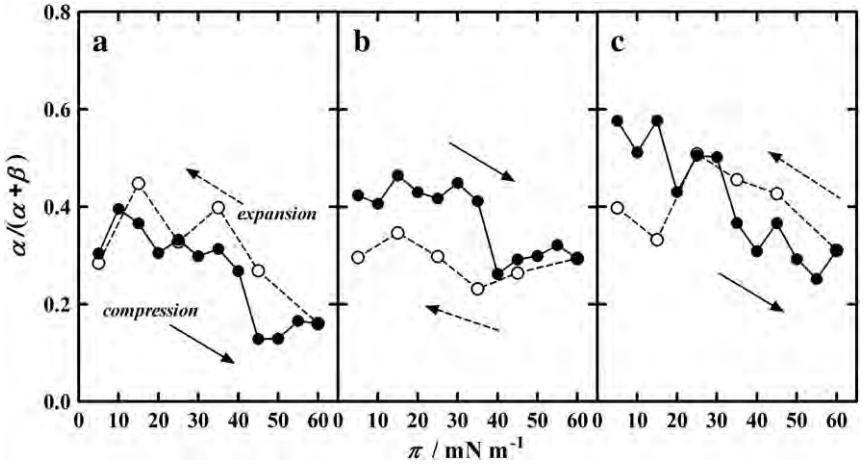

Fig. 8. Peak area ratio, $\alpha/(\alpha+\beta)$, of the amide I band intensity for ~1650 cm^{-1}/(~1650 + ~1620) cm^{-1} against surface pressure (π) during compression (filled circles and solid lines) and expansion (open cycles and dashed lines). The peak at ~1650 cm^{-1} is assigned to the α-helical secondary structure and the peak at ~1620 cm^{-1} is assigned to the antiparallel β-sheet. (a) DPPC/PA(=90:9, wt/wt)/Hel 13–5, (b) DPPC/PG(=68:22, wt/wt)/Hel 13–5, and (c) DPPC/PG/PA(=68:22:9, wt/wt/wt)/Hel 13–5 at $X_{Hel\ 13-5}=0.1$.

monolayers and multilayers are not fully discussed. The proteins have several α-helical moieties with different amphiphilicity, hydrophobicity, and amino acid residues in a molecule. Therefore, intramolecular interactions of the proteins such as hydrogen bonding, S–S bonding as a linkage of the moieties, van der Waals force, and electrostatic force among the α-helical parts complicate the above-mentioned issues. To overcome the issues (besides developing a new medicine against the neonatal RDS patients), several analogous peptides of the proteins' α-helical moieties, which are designed as a mimicry of one of the α-helices, have been utilized (e.g., KL_4[19], $SP\text{-}B_{1\text{-}25}$[54], and Hel 13–5[21]). Thus, the three- or four-component systems including DPPC, PG, PA, and Hel 13–5 provide a useful model for in vitro biophysical studies of the surface-associated reservoirs that are formed during compression and expansion cycles in the lungs. The previous studies of surface-associated reservoirs in the PS model systems including Hel 13–5 have clarified the existing location and formation of them employing π—A and ΔV—A isotherms, in situ fluorescence microscopy, and AFM [9,21]. The preparations with the other peptide analogues have also revealed that the reservoirs form at around 40 mN m^{-1} [7,10]. Morrow et al. have suggested from NMR investigations on interaction between PG and SP-C that positively charged parts of SP-C are located near the bilayer surface [55]. In more recent work, Mendelson and co-workers have quantitatively revealed the multilayer transition in the DPPC/DPPG/SP-C system using the IR spectroscopy of films transferred at continuously varying surface pressure [56]. In the report, the formation of reservoirs induced by surface pressure is possibly based on the intermolecular interaction between the positively charged protein (or peptide) and the negatively charged phospholipid such as PG.

The emergence of reservoirs causes a hysteresis in π—A and ΔV—A isotherms as well as spectrum parameters regarding lipid orientations and protein (or peptide) secondary structures during the compression–expansion cycling. That is, it is suggested that the formation and function of reservoirs across the surface are controlled not only by the electrostatic attraction between lipids and peptide but also by the structural transition of proteins. This transition is considered to be induced by destruction of the hydrogen and S–S bonding constructing protein structures. In the in vitro monolayer study, the destructive factors are typically an applied surface pressure and an environmental lipid (especially, its hydrocarbon chains). It is previously found that single Hel 13–5 monolayers in the absence of lipids at the air–water interface are in ~70% α-helical structure irrespective of surface pressure [26]. However, over-compression above the collapse pressure decreases the α-helix ratio by ~20%. In the presence of DPPC, the secondary structure of Hel 13–5 monolayers transform almost fully to β-sheet upon compression up to the collapse pressure. That is, considering surface composition becoming enriched in DPPC upon compression, and thus lipid squeeze-out of the other components, it is found that the secondary structure transition is mainly induced by DPPC left at the interface. Cai et al. have indicated the irreversible interconversion of KL_4 peptide in the phospholipid mixtures [27]. Flach and coworkers [57] have reported the conversion from α-helix to β-sheet for $SP\text{-}B_{9\text{-}36}$ peptide in the binary DPPG system. That is, the protein structure is strongly deformed by environmental lipid densities (especially phospholipids with saturated hydrocarbon chains, e.g., DPPC) rather than applied surface pressures. As expected easily, the lipid species such as PG and PA are also considered to be an important factor for deformation of the secondary structure. In the present study, the addition of PA and PG to the DPPC/Hel 13–5 mixture improves the relative α-helical contents compared with the binary DPPC/Hel 13–5 system (Fig. 8). These results lead to the following findings: (1) the hydrogen bonding to construct the secondary structure of Hel 13–5 is perturbed mainly by DPPC and (2) the surface-associated reservoir including charged PA and PG disturbs the interconversion of the secondary structure. Regarding (2), in particular, PA prevents to small extents Hel 13–5 α-helix structures from transforming to the β-sheet and facilitates the recovery of the secondary structures to α-helix. On the other hand, PG sustains the higher α-helix ratio at low surface pressures and assumes stronger resistance to the interconversion to the β-sheet during the compression. The carboxyl group in PA molecules is partially dissociated by 30–40% under the current condition [11]. Thus, a switching motion between COOH and COO^- is considered to be an effective driving force for the recovery of Hel 13–5 secondary structure from the β-sheet and for the release of surface-associated reservoirs onto the interface during expansion. Considering the predominant α-helical structure of Hel 13–5 in the aqueous solutions containing phospholipids [24] and in the bilayer form (Fig. 1), it can be suggested that the surface-associated reservoir exerts prevention of the protein structure transition (or surface denature) by incorporating the proteins into the reservoir.

5. Conclusion

The multi-component pulmonary surfactant mimics, which contain an SP-B analogous peptide (Hel 13–5), have been investigated using the ATR-FTIR and the in situ PM-IRRAS techniques. The ATR-FTIR measurement reveals that Hel 13–5 adopts mainly α-helical structure in the binary and ternary lipid films made of DPPC, PG, and PA. In the in situ PM-IRRAS measurement, the transition of Hel 13–5 secondary structure from α-helix to β-sheet takes place during the monolayer compression. The α-helix recovers quantitatively upon expansion, whereas the α-helical ratio shows a hysteresis during the cycle. On the other hand, the peak intensity and wavenumber

of ν_a (CH_2) mode based on hydrophobic chains of the lipids also indicate the hysteresis behavior, which is deeply related to the formation of surface-associated reservoirs at high surface pressures. It is commonly accepted that the reservoir formation generates a hysteresis to physical parameters during the cycle to minimize the work of breathing. Besides the function, however, the current study has additionally suggested preservation of the α-helical structure of proteins. This confidence warrants further function on distribution, location, and transition of protein structures employing other techniques and methods. Nevertheless, the in situ PM-IRRAS results here reveal the facts that the release of squeezed-out lipids and peptides from the surface-associated reservoir is accelerated by partially charged PA molecules and that PG assumes a strong resistance to transition of the peptide structure upon compression.

Acknowledgements

This work was supported by a Grant-in-Aid for Scientific Research 23510134 from the Japan Society for the Promotion of Science (JSPS). This work was also supported by a Grant-in-Aid for Young Scientists (B) 22710106 from JSPS and by a Foundation from Oil&Fat Industry Kaikan (H.N.).

Appendix A. Supplementary data

Supplementary data to this article can be found online at http://dx.doi.org/10.1016/j.bbamem.2013.01.003.

References

[1] S. Schürch, J. Goerke, J.A. Clements, Direct determination of surface tension in the lung, Proc. Natl. Acad. Sci. U. S. A. 73 (1976) 4698–4702.
[2] S. Schürch, R. Qanbar, H. Bachofen, F. Possmayer, The surface-associated surfactant reservoir in the alveolar lining, Biol. Neonate 67 (Suppl. 1) (1995) 61–76.
[3] S. Schürch, F.H.Y. Green, H. Bachofen, Formation and structure of surface films: captive bubble surfactometry, Biochim. Biophys. Acta 1408 (1998) 180–202.
[4] D. Follows, F. Tiberg, R.K. Thomas, M. Larsson, Multilayers at the surface of solutions of exogenous lung surfactant: direct observation by neutron reflection, Biochim. Biophys. Acta 1768 (2007) 228–235.
[5] M. Amrein, A. von Nahmen, M. Sieber, A scanning force- and fluorescence light microscopy study of the structure and function of a model pulmonary surfactant, Eur. Biophys. J. 26 (1997) 349–357.
[6] S. Krol, M. Ross, M. Sieber, S. Kunneke, H.-J. Galla, A. Janshoff, Formation of three-dimensional protein-lipid aggregates in monolayer films induced by surfactant protein B, Biophys. J. 79 (2000) 904–918.
[7] D.Y. Takamoto, M.M. Lipp, A. Von Nahmen, K.Y.C. Lee, A.J. Waring, J.A. Zasadzinski, Interaction of lung surfactant proteins with anionic phospholipids, Biophys. J. 81 (2001) 153–169.
[8] H. Nakahara, S. Lee, G. Sugihara, O. Shibata, Mode of interaction of hydrophobic amphiphilic α-helical peptide/dipalmitoylphosphatidylcholine with phosphatidylglycerol or palmitic acid at the air–water interface, Langmuir 22 (2006) 5792–5803.
[9] H. Nakahara, S. Lee, O. Shibata, Pulmonary surfactant model systems catch the specific interaction of an amphiphilic peptide with anionic phospholipid, Biophys. J. 96 (2009) 1415–1429.
[10] J. Pérez-Gil, C. Casals, D. Marsh, Interactions of hydrophobic lung surfactant proteins SP-B and SP-C with dipalmitoylphosphatidylcholine and dipalmitoylphosphatidylglycerol bilayers studied by electron spin resonance spectroscopy, Biochemistry 34 (1995) 3964–3971.
[11] H. Nakahara, S. Lee, Y. Shoyama, O. Shibata, The role of palmitic acid in pulmonary surfactant systems by Langmuir monolayer study: lipid–peptide interactions, Soft Matter 7 (2012) 11351–11359.
[12] S.-H. Yu, F. Possmayer, Lipid compositional analysis of pulmonary surfactant monolayers and monolayer-associated reservoirs, J. Lipid Res. 44 (2003) 621–629.
[13] P. Krüger, J.E. Baatz, R.A. Dluhy, M. Lösche, Effect of hydrophobic surfactant protein SP-C on binary phospholipid monolayers. Molecular machinery at the air/water interface, Biophys. Chem. 99 (2002) 209–228.
[14] R. Veldhuizen, K. Nag, S. Orgeig, F. Possmayer, The role of lipids in pulmonary surfactant, Biochim. Biophys. Acta 1408 (1998) 90–108.
[15] J.C. Clark, S.E. Wert, C.J. Bachurski, M.T. Stahlman, B.R. Stripp, T.E. Weaver, J.A. Whitsett, Targeted disruption of the surfactant protein B gene disrupts surfactant homeostasis, causing respiratory failure in newborn mice, Proc. Natl. Acad. Sci. U. S. A. 92 (1995) 7794–7798.
[16] L.M. Nogee, G. Garnier, H.C. Dietz, L. Singer, A.M. Murphy, D.E. deMello, H.R. Colten, A mutation in the surfactant protein B gene responsible for fatal neonatal respiratory disease in multiple kindreds, J. Clin. Invest. 93 (1994) 1860–1863.
[17] P.L. Ballard, L.M. Nogee, M.F. Beers, R.A. Ballard, B.C. Planer, L. Polk, D.E. deMello, M.A. Moxley, W.J. Longmore, Partial deficiency of surfactant protein B in an infant with chronic lung disease, Pediatrics 96 (1995) 1046–1052.
[18] S.D. Revak, T.A. Merritt, C.G. Cochrane, G.P. Heldt, M.S. Alberts, D.W. Anderson, A. Kheiter, Efficacy of synthetic peptide-containing surfactant in the treatment of respiratory distress syndrome in preterm infant rhesus monkeys, Pediatr. Res. 39 (1996) 715–724.
[19] J. Ma, S. Koppenol, H. Yu, G. Zografi, Effects of a cationic and hydrophobic peptide, KL4, on model lung surfactant lipid monolayers, Biophys. J. 74 (1998) 1899–1907.
[20] T.E. Wiswell, R.M. Smith, L.B. Katz, L. Mastroianni, D.Y. Wong, D. Willms, S. Heard, M. Wilson, R.D. Hite, A. Anzueto, S.D. Revak, C.G. Cochrane, Bronchopulmonary segmental lavage with Surfaxin (KL(4)-surfactant) for acute respiratory distress syndrome, Am. J. Respir. Crit. Care Med. 160 (1999) 1188–1195.
[21] H. Nakahara, S. Lee, G. Sugihara, C.-H. Chang, O. Shibata, Langmuir monolayer of artificial pulmonary surfactant mixtures with an amphiphilic peptide at the air/water interface: comparison of new preparations with Surfacten (Surfactant TA), Langmuir 24 (2008) 3370–3379.
[22] A. Kitamura, T. Kiyota, M. Tomohiro, A. Umeda, S. Lee, T. Inoue, G. Sugihara, Morphological behavior of acidic and neutral liposomes induced by basic amphiphilic α-helical peptides with systematically varied hydrophobic-hydrophilic balance, Biophys. J. 76 (1999) 1457–1468.
[23] H. Nakahara, S. Nakamura, T. Hiranita, H. Kawasaki, S. Lee, G. Sugihara, O. Shibata, Mode of interaction of amphiphilic α-helical peptide with phosphatidylcholines at the air–water interface, Langmuir 22 (2006) 1182–1192.
[24] T. Kiyota, S. Lee, G. Sugihara, Design and synthesis of amphiphilic α-helical model peptides with systematically varied hydrophobic-hydrophilic balance and their interaction with lipid- and bio-membranes, Biochemistry 35 (1996) 13196–13204.
[25] S. Lee, T. Furuya, T. Kiyota, N. Takami, K. Murata, Y. Niidome, D.E. Bredesen, H.M. Ellerby, G. Sugihara, De novo-designed peptide transforms Golgi-specific lipids into Golgi-like nanotubules, J. Biol. Chem. 276 (2001) 41224–41228.
[26] H. Nakahara, S. Lee, O. Shibata, Specific interaction restrains structural transitions of an amphiphilic peptide in pulmonary surfactant model systems: An in situ PM-IRRAS investigation, Biochim. Biophys. Acta 1798 (2010) 1263–1271.
[27] P. Cai, C.R. Flach, R. Mendelsohn, An infrared reflection–absorption spectroscopy study of the secondary structure in (KL4)4K, a therapeutic agent for respiratory distress syndrome, in aqueous monolayers with phospholipids, Biochemistry 42 (2003) 9446–9452.
[28] X. Bi, C.R. Flach, J. Perez-Gil, I. Plasencia, D. Andreu, E. Oliveira, R. Mendelsohn, Secondary structure and lipid interactions of the N-terminal segment of pulmonary surfactant SP-C in Langmuir films: IR reflection–absorption spectroscopy and surface pressure studies, Biochemistry 41 (2002) 8385–8395.
[29] M. Gustafsson, M. Palmblad, T. Curstedt, J. Johansson, S. Schurch, Palmitoylation of a pulmonary surfactant protein C analogue affects the surface associated lipid reservoir and film stability, Biochim. Biophys. Acta 1466 (2000) 169–178.
[30] M. Gustafsson, G. Vandenbussche, T. Curstedt, J.M. Ruysschaert, J. Johansson, The 21-residue surfactant peptide (LysLeu4)4Lys(KL4) is a transmembrane alpha-helix with a mixed nonpolar/polar surface, FEBS Lett. 384 (1996) 185–188.
[31] Y. Tanaka, T. Takei, T. Aiba, K. Masuda, A. Kiuchi, T. Fujiwara, Development of synthetic lung surfactants, J. Lipid Res. 27 (1986) 475–485.
[32] T. Furuya, T. Kiyota, S. Lee, T. Inoue, G. Sugihara, A. Logvinova, P. Goldsmith, H.M. Ellerby, Nanotubules formed by highly hydrophobic amphiphilic a-helical peptides and natural phospholipids, Biophys. J. 84 (2003) 1950–1959.
[33] S. Frey, L.K. Tamm, Orientation of melittin in phospholipid bilayers. A polarized attenuated total reflection infrared study, Biophys. J. 60 (1991) 922–930.
[34] A. Menikh, M.T. Saleh, J. Gariépy, J.M. Boggs, Orientation in lipid bilayers of a synthetic peptide representing the C-terminus of the A1 domain of shiga toxin. A polarized ATR-FTIR study, Biochemistry 36 (1997) 15865–15872.
[35] P.H. Axelsen, M.J. Citra, Orientational order determination by internal reflection infrared spectroscopy, Prog. Biophys. Mol. Biol. 66 (1996) 227–253.
[36] U.P. Fringeli, H.H. Günthard, Infrared membrane spectroscopy, Springer-Verlag, New York, 1981.
[37] S.A. Tatulian, Attenuated total reflection Fourier transform infrared spectroscopy: a method of choice for studying membrane proteins and lipids, Biochemistry 42 (2003) 11898–11907.
[38] D. Marsh, T. Páli, Infrared dichroism from the X-ray structure of bacteriorhodopsin, Biophys. J. 80 (2001) 305–312.
[39] D. Marsh, Orientation and peptide-lipid interactions of alamethicin incorporated in phospholipid membranes: polarized infrared and spin-label EPR spectroscopy, Biochemistry 48 (2009) 729–737.
[40] D. Marsh, M. Müller, F.J. Schmitt, Orientation of the infrared transition moments for an α-helix, Biophys. J. 78 (2000) 2499–2510.
[41] H. Nakahara, O. Shibata, Y. Moroi, Examination of surface adsorption of cetyltrimethylammonium bromide and sodium dodecyl sulfate, J. Phys. Chem. B 115 (2011) 9077–9086.
[42] M.S. Vinchurkar, K.H. Chen, S.S. Yu, S.J. Kuo, H.C. Chiu, S.H. Chien, S.I. Chan, Polarized ATR-FTIR spectroscopy of the membrane-embedded domains of the particulate methane monooxygenase, Biochemistry 43 (2004) 13283–13292.
[43] R. Mendelsohn, J.W. Brauner, A. Gericke, External infrared reflection absorption spectrometry of monolayer films at the air–water interface, Annu. Rev. Phys. Chem. 46 (1995) 305–334.
[44] E. Maltseva, V.L. Shapovalov, H. Möhwald, G. Brezesinski, Ionization State and Structure of L-1,2-Dipalmitoylphosphatidylglycerol Monolayers at the Liquid/Air Interface, J. Phys. Chem. B 110 (2006) 919–926.
[45] C.R. Flach, P. Cai, D. Dieudonne, J.W. Brauner, K.M.W. Keough, J. Stewart, R. Mendelsohn, Location of structural transitions in an isotopically labeled lung surfactant SP-B peptide by IRRAS, Biophys. J. 85 (2003) 340–349.

[46] A. Kerth, A. Erbe, M. Dathe, A. Blume, Infrared reflection absorption spectroscopy of amphipathic model peptides at the air/water interface, Biophys. J. 86 (2004) 3750–3758.
[47] S. Shanmukh, P. Howell, J.E. Baatz, R.A. Dluhy, Effect of hydrophobic surfactant proteins SP-B and SP-C on phospholipid monolayers. Protein structure studied using 2D IR and $\beta\nu$ correlation analysis, Biophys. J. 83 (2002) 2126–2141.
[48] D. Blaudez, T. Buffeteau, J.C. Cornut, B. Desbat, N. Escafre, M. Pezolet, J.M. Turlet, Polarization-modulated FT-IR spectroscopy of a spread monolayer at the air/water interface, Appl. Spectrosc. 47 (1993) 869–874.
[49] H. Nakahara, A. Dudek, Y. Nakamura, S. Lee, C.H. Chang, O. Shibata, Hysteresis behavior of amphiphilic model peptide in lung lipid monolayers at the air–water interface by an IRRAS measurement, Colloids Surf. B 68 (2009) 61–67.
[50] A. Gericke, H. Hühnerfuss, In situ investigation of saturated long-chain fatty acids at the air/water interface by external infrared reflection–absorption spectrometry, J. Phys. Chem. 97 (1993) 12899–12908.
[51] X. Wen, J. Lauterbach, E.I. Franses, Surface densities of adsorbed layers of aqueous sodium myristate inferred from surface tension and infrared reflection absorption spectroscopy, Langmuir 16 (2000) 6987–6994.
[52] M.M. Lipp, K.Y.C. Lee, D.Y. Takamoto, J.A. Zasadzinski, A.J. Waring, Coexistence of buckled and flat monolayers, Phys. Rev. Lett. 81 (1998) 1650–1653.
[53] A.V. Nahmen, M. Schenk, M. Sieber, M. Amrein, The structure of a model pulmonary surfactant as revealed by scanning force microscopy, Biophys. J. 72 (1997) 463–469.
[54] S.L. Frey, L. Pocivavsek, A.J. Waring, F.J. Walther, J.M. Hernandez-Juviel, P. Ruchala, K.Y. Lee, Functional importance of the NH_2-terminal insertion sequence of lung surfactant protein B, Am. J. Physiol. Lung Cell. Mol. Physiol. 298 (2010) L335–L347.
[55] M.R. Morrow, S. Taneva, G.A. Simatos, L.A. Allwood, K.M.W. Keough, Deuterium NMR studies of the effect of pulmonary surfactant SP-C on the 1,2-dipalmitoyl-*sn*-glycero-3-phosphocholine headgroup: a model for transbilayer peptides in surfactant and biological membranes, Biochemistry 32 (1993) 11338–11344.
[56] G. Mao, J. Desai, C.R. Flach, R. Mendelsohn, Structural characterization of the monolayer-multilayer transition in a pulmonary surfactant model: IR studies of films transferred at continuously varying surface pressures, Langmuir 24 (2008) 2025–2034.
[57] D. Dieudonné, R. Mendelsohn, R.S. Farid, C.R. Flach, Secondary structure in lung surfactant SP-B peptides: IR and CD studies of bulk and monolayer phases, Biochim. Biophys. Acta 1511 (2001) 99–112.